

SCATTERED LIGHT IN THE FOS: AN ASSESSMENT USING SCIENCE DATA

Michael R. Rosa ¹

The Space Telescope European Coordinating Facility
European Southern Observatory, D-85747 Garching, Germany

FOS Instrument Science Report CAL/FOS-114

October 1993

Adapted and revised from an article first published
in the ST-ECF Newsletter No. 20, p. 16-19, August 1993

Abstract

The Faint Object Spectrograph (FOS) uses a truly one-dimensional detector and so source and the background signal - sky and internal - usually cannot be observed strictly simultaneously. In this analysis, some 360 individual exposures of a large variety of target types and magnitudes have been inspected in two FOS modes that do provide simultaneous background recording, namely BLUE side detector with grating G130H and AMBER detector with grating G780H. Residual counts in portions of the diode array that cover the wavelength ranges with near zero sensitivity seem to originate from at least two sources.

The charged particle induced background is usually about 30 % stronger than predicted by the calibration currently in use in the standard pipeline reduction. In addition, bright red targets show the presence of a considerable amount of diffuse scattered light in the spectrograph. The data suggest that mirror-imaged ghost spectra are of no concern. An empirical model incorporating both of the former cases is shown to match the observational data. Prescriptions for recalibration of FOS BLUE, G130H data are given and the impact on the final calibrated fluxes demonstrated.

I. Introduction

For low resolution spectrophotometry, one of the huge advantages of the HST over ground-based telescopes is the absence of night sky light originating within or scattered by the Earth's atmosphere. Clearly, astronomical background light of Galactic or zodiacal origin or from within the aperture directed at a point source located in an extended target, will be suppressed substantially only by using very small entrance apertures. This capability can be fully exploited after the COSTAR servicing mission late this year. In order to achieve the limiting performance set by these sources, any non-astronomical signal originating behind the spectrograph entrance aperture must be determined and subtracted. Usually being subsumed under the terms "dark" or "background" in the FOS literature, these internal sources of unwanted signal have the following origins:

- Non-science counts generated within the detector or its environment. These are produced by thermionic emission within the detector and by high energy cosmic particles which induce Čerenkov emission.

¹Affiliated to the Astrophysics Division of the Space Science Department of the European Space Agency

- Grating scatter. The FOS is a single pass spectrometer with blazed, concave gratings. Both the blue and the red side cover wide spectral ranges. Therefore the FOS, like many ground-based low resolution spectrographs, is subject to scattered light.
- Ghosts. Since the FOS detectors are covered with face-plates, de-focussed ghost images of the illuminated detector array can be produced.

II. Pre-launch and in-flight calibration

Between 1983 and the launch of HST in 1990, the numerous tests and ground calibrations performed by the FOS Investigation Definition Team (IDT) were presented in a series of FOS Instrument Science Reports (ISR; CAL/FOS).

During the orbital and science verification phases (OV/SV), 17 major aspects of the FOS calibration were assessed: these are summarised in the FOS Science Verification Report, 1992. These investigations showed the following behaviour. Thermionic detector background as measured in the thermal-vacuum ground test is of order 0.0003 ct/s/diode (Beaver & Lyons, 1992, CAL/FOS-076). This is well below specification and at least an order of magnitude below other sources of background.

In-orbit dark measurements during OV/SV showed a mean background level of about 0.007 ct/s/diode in the blue detector and about 0.01 in the red side detector, ie, a factor of 30 above the pure thermionic noise. The source of this background is Čerenkov light induced in the detector faceplates by high energy particles present at the altitude of the HST orbit. This background can be expected to vary substantially with orbital parameters and time. Indeed, besides its burst-like character it appears to scale with geomagnetic latitude and possibly also with longitude (see CAL/FOS-080).

As a zero-order correction for exposures taken without dedicated background observations, the standard pipeline reduction performed at STScI uses a model of this background based on these OV/SV data. The model consists of a 3rd order polynomial for the blue detector and 2 separate 3rd order polynomials for the red detector. These background spectra are scaled using a factor derived from the variation of background level with geomagnetic latitude determined using the dark exposures obtained in 1990.

Pre-launch laboratory measurements using sequences of cut-on filters with tungsten lamp illumination of the apertures had shown a large susceptibility to diffuse scattered light in both the blue and red channel. Counts received in the wavelength range 1600 Å to 2300 Å (grating G190H) were almost entirely due to photons with effective wavelengths between 3500 Å and 5500 Å (CAL/FOS-005 and 012a). Other indications of scattered light in the dispersion direction are found in anomalous excess blue light reported in CAL/FOS-011 and CAL/FOS-059. These tests were designed originally to measure scattered light perpendicular to the dispersion direction. Finally, a comparison of in-orbit spectra of a solar-type star (16 Cyg B) taken with FOS and with the solar-blind GHRS show the large amount of red scattered light in the FOS spectra below 2100 Å (Caldwell & Cunningham, 1992; see also Kinney (1993), Appendix D of the FOS Instrument Handbook V4).

Pre-launch calibration data may have shown ghosts in exposures of the Pt-Cr-Ne wavelength calibration lamp with grating G130H. Below the 1150 Å cut-off of the MgF₂ face-plate, a number of unidentified emission lines were found with count rates about a hundredth of those of the primary calibration spectrum in the long wavelength part of the G130H spectral range (CAL/FOS-012a).

III. Analysis of archival science data

How large are the effects on science data taken with FOS? Although tests with non-astronomical light sources are able to generate the majority of calibration data, only the analysis of data of

real astronomical sources with well-known spectra can show whether all adverse effects are under control. Since the FOS detectors are one-dimensional arrays, background data can never be taken truly simultaneously with the target spectra over the full wavelength range covered by a particular grating/detector combination. For the high dispersion mode there are, however, two exceptions. The MgF_2 face-plate of the blue detector becomes opaque at around 1150 \AA . The signal observed in the wavelength range 1080 to 1150 \AA in exposures with the blue detector and the G130H grating should, therefore, represent a very good estimate of a truly simultaneous background recording. Similarly, the quantum efficiency of the red detector becomes exceedingly low longward of 8600 \AA , so that data on faint blue objects taken with the red detector and G780H combination should consist essentially of non-astronomical background between about 8600 and 9220 \AA . The situation for blue train spectra is sketched in Figure 1.

By March 1993 there were about 350 spectrophotometric exposures of scientific targets in the HST Archive with the blue detector + G130H combination, but only a few with the red detector and G780H. In the following therefore, only the analysis of the blue data is described. It is based on raw count rates, corrected for pulse overlap, GIMP and dead-diode effects, ie, the *.c4h* files of the standard reduction pipeline. After interpretation of the background on individual spectra, three quantities were derived for each using an automated MIDAS procedure which also extracted all essential exposure information from the data headers. These three quantities which are illustrated in Figure 1 are:

- **B:** the average observed count rate (ct/s/diode) in diodes 1–45 corresponding to the range 1087 to 1132 \AA . The upper wavelength limit was chosen well below the nominal MgF_2 window edge (having used UV bright targets to confirm the cut-off).
- **S:** the average signal + background count rate in diodes 471 to 511 as a measure of the primary signal strength to test for mirror imaged ghosts onto the 1–45 diode region.
- **P:** the average predicted background rate in diodes 1–45, taken from the pipeline product *.c7h* file, ie. the modelled particle induced background level used in the pipeline reduction.

Three categories of targets can be identified – critical in terms of impact on the scientific data and informative in terms of a possible separation of the three suspected background sources – namely particle induced, grating scatter and ghosts. Three classes of target spectrum will illustrate the various effects.

Faint targets with blue spectra If the count rates due to the intrinsic target spectrum are comparable to the in-orbit particle background rate of 0.007 ct/s/diode , the determination of the intrinsic energy distribution critically depends upon the ability to correctly predict the actual background. For such faint blue targets, any grating scatter and ghosts are orders of magnitude weaker than the particle background. Ideally, if the background model is fully applicable, the ratio $R = \mathbf{B/P}$ should then be unity.

The inset in Figure 2 shows a spectrum typical for this category – here the integrated energy distribution of numerous OB stars in a giant H II region. The sharp decline in target signal caused by the entrance window below the Geocoronal Ly α emission line can be clearly seen. It is obvious that the predicted background level falls short of the actually observed rate, here by about 30 % ($R = 1.30$). The rest of Figure 2 shows versions of the fully calibrated energy distribution from these data using the model predicted background level (pipeline version), and using the same background scaled up by 30 % to match the observed level in the first 45 diodes. The unnatural rise of the “pipeline version” at wavelengths below 1250 \AA is a result of the underestimation of the background. The model is an appropriately combined and reddened set of Kurucz model atmospheres.

Red targets with intrinsically faint blue spectra The signal shortward of 1150 Å is composed of the actual particle induced background as discussed above plus photons scattered from the grating: these originate predominantly in the range 3000 to 5500 Å . For intrinsically bright red targets the latter component can be overwhelming. Presumably it has a flat distribution but since this background can only be assessed in the first 45 diodes, its actual shape remains unknown. Only cross-instrument comparison of GHRs and FOS data on the same star and/or a comparison with predicted data using stellar atmosphere models and interstellar extinction laws can give more insight.

Bright blue targets The signal below 1150 Å consists of particle induced background, scattered light from photons in the 3000 to 5500 Å range and, potentially, a measurable signal due to ghosts. Well exposed spectra of AGN's with red-shifted C IV 1550 Å emission lines do suggest, however, that ghosts imaged in reverse about the approximate center of the diode array with a scale factor near 1.0 cannot be much stronger than 1/300 the intensity of the primary signal.

IV. Discussion

There are thus two significant contributors to the background level observed in the FOS BLUE, G130H mode. Firstly, we see the anticipated particle induced Čerenkov light at levels in excess of the predictions from the model used in the standard data calibration pipeline. Secondly, grating scatter of light from the spectral range 3000 to 5500 Å . This is illustrated for the full sample of relevant science data in the HST archive up to March 1993 in Figure 3. On a logarithmic scale are shown the values **B** (measured background below 1137 Å) versus **S** (measured signal + background above 1560 Å), grouped into different target categories (see legend). Also shown are the values of the background predicted in the pipeline reduction as horizontal dashes. The continuous lines represent empirical models of the background as described in the Appendix.

Faint and very faint targets are found at count rates below 0.3 ct/s/diode or $\log S \leq -0.5$. As can be seen, all measurements of the background level, even those for the faintest targets are larger than the predicted ones. Apparently the in-orbit background prediction falls short of the actual values by an average factor 1.3 .

For targets with appreciable flux at wavelengths above 1560 Å , **B** is a nearly linear function of **S**, with scale coefficients depending on target type: very red solar-type spectra, A and F stars, OB stars and AGN can be easily distinguished. This is clear evidence for grating scatter of photons at wavelengths outside the range imaged by the G130H grating. The tight relations do suggest that correction formulae can be derived if the spectral energy distribution in the wavelength range 1600 to 5500 Å is well known.

V. Suggestions for recalibrating G130H data

The background level in FOS BLUE, G130H mode observations can be successfully modelled by scaling up the particle background component predicted from the model currently used in the pipeline and adding a component due to diffuse scattering of photons in the wavelength range 3000 to 5500 Å . Since the scattered light component is very likely to be constant across the detector, the improved background **b'** as a function of location on the detector can be estimated for each individual exposure with sufficient accuracy by the following formulae:

(a) Faint targets, background dominated by Čerenkov light

$$\mathbf{b}'(\text{diode}) = g \times \mathbf{P}(\text{diode}) \quad ; \quad g = \mathbf{B}(1-45) / \mathbf{P}(1-45)$$

(b) Bright and/or red targets, background dominated by scattered light

$$\mathbf{b}'(\text{diode}) = 1.3 \times \mathbf{P}(\text{diode}) + c \quad ; \quad c = \mathbf{B}(1-45) - 1.3 \times \mathbf{P}(1-45)$$

Currently there is no parameter in the calibration header keywords that would allow the *calfos* task in the STSDAS *fos* package to scale the internal background model according to the above formulae. The present experiments with background recalibration have been done in MIDAS using table files holding in separate columns the wavelengths, the GIMP and dead diode corrected count rates, the pipeline background, the flat field and the inverse sensitivity, generated from the highest group of the calibrated data set FITS files. Recalibrated fluxes have then been obtained using the equation

$$flux = (counts \times adjusted\ background) \times flat \times inverse\ sensitivity$$

Workarounds in STSDAS are possible either by substituting a fake double aperture observation or using a combination of the calibration switches on several partially calibrated iterations. In the former case the new background (de-corrected for flat field) has to be inserted as data for the second aperture (interleaving with the first aperture in a N*2 group sized file). The header keywords have to be modified to signal double aperture observations and calibration reference file pointers have to be copied into the second aperture keywords accordingly.

Presumably the gain factor $g = 1.3$ found here for the pipeline modelled particle background is valid for other grating combinations with the blue detector calibrated with the reference files *b3m1128my.r0h* and *ba31407ly.cy8*. In fact, a model of the background with $g = 1.0$ can be obtained using the results of CAL/FOS-080 (Lyons et al. 1992) instead, augmented by a fit to residuals in geomagnetic longitude. A preliminary result of $g \approx 1.3$ has also been found here for FOS RED, G780H. This is indicative only due to the small database available.

For all relevant cases, however, scaling of the background according to the above formula is sufficient, and for faint targets allowance for the scale factor in the particle background alone may be adequate for other grating modes. However, the amount of scattering in these modes (G190H, G270H etc.) is not known and cannot be assessed directly in the way done here for G130H. Probably a boot strap method could be used by first correcting the G130H observations as shown here. In further steps observations in G190H and so on could be corrected for in-orbit dark and scattered light using the wavelengths overlap with the previous grating ranges.

Recommendations for an improved background correction have also been given by Kinney and Bohlin (1993). Their findings are in good agreement with the analysis presented here.

To conclude and in order to demonstrate the significance of the background correction, the spectral energy distribution of a F0 Iab type star is shown in two versions (pipeline result and recalibrated) in Figure 4. The comparison with a reddened and scaled Kurucz model atmosphere should be indicative only, because the latter does not include chromospheric emission apparently present in the data.

References

- Beaver, E.A. and Lyons, R.W.: 1992, CAL/FOS-076
- Caldwell, J. and Cunningham, C.C.: 1992, Science Verification 1343 Inetrim Report
- Kinney, A.L.: 1993, FOS Instrument Handbook V.4
- Kinney, A.L. and Bohlin, R.C.: 1993, CAL/FOS-103
- Lyons, R.W., Linsky, J.B., Beaver, E.A., Baity, W.A. and Rosenblatt, E.J.: 1992, CAL/FOS-80

Appendix: An empirical background model

An empirical model which matches the data for bright targets (ie. signal large compared to pipeline predicted background) and provides simultaneously a lower limit to the very faint target data has the form:

$$b = g \times P + f \times (S - g \times P)$$

- b** estimate of total background **B** at 1100 Å
- g** gain factor for predicted particle background **P**
- f** scale factor for scattered light
- S** signal + background at 1600 Å

Fits to science data in the HST archive yield the following parameter sets for various classes of target spectra

Spectrum	g	f	cases
G,K,M stars	1.3	0.440 ± 0.090	27
A,F stars	1.3	0.032 ± 0.006	11
O,B stars	1.3	0.010 ± 0.002	38
AGN	1.3	0.007 ± 0.001	16
very faint targets	1.3	undetermined	83

The entry G,K,M stars also includes observations of solar system bodies. The low value of f for AGN presumably reflects the fact that the wavelength range used to determine **S** incorporates the redshifted C IV emission line. Given that no individual corrections for interstellar extinction have been made and that targets have been assigned to very loosely defined groups, the tightness of the relations is surprising. This fact also argues in favour of a diffuse scattering mechanism rather than ghost images where spectral features differ from one target to the next even within one grouping. For very faint targets, solar stray light in the OTA could be an additional source of background excess. However, the residuals $(B - b)/P$ do not show any significant correlation with any of the three relevant orbital parameters Sun angle, Moon angle or elevation of Sun above horizon during observation.

Figure captions

Figure 1 : A sketch of raw data in the FOS BLUE, G130 mode for a faint, blue target. Because of diminishing sensitivity, the target signal weakens towards the MgF_2 window cut-off at 1150 \AA . The Geocoronal $\text{Ly } \alpha$ and O I emission lines are the dominant sky features. The quantities discussed in the text, namely background level predicted (**P**) and observed (**B**), as well as signal (**S**), are indicated.

Figure 2 : A faint, blue target - integrated light from an OB cluster in an external galaxy. Flux calibrated data in the pipeline version are compared with the recalibrated product and a population synthesis model. The upturn of the pipeline energy distribution shortward of $\text{Ly } \alpha$ is unphysical and a result of background underestimation. The insert shows the raw counts with the pipeline prediction of background.

Figure 3 : The signal vs. background diagram for FOS BLUE, G130H observations. Note that all observed background levels are in excess of the pipeline predictions. The models shown predict background including a scaled particle induced background and an off-order grating scatter contribution scaling with the number of red photons available. The close grouping of the different spectral types is quite remarkable.

Figure 4 : The effect of background underestimation on a far-UV spectrum of an intrinsically red and bright target (an F0 supergiant). The model is a Kurucz atmosphere and the excess at short wavelengths could be chromospheric emission.

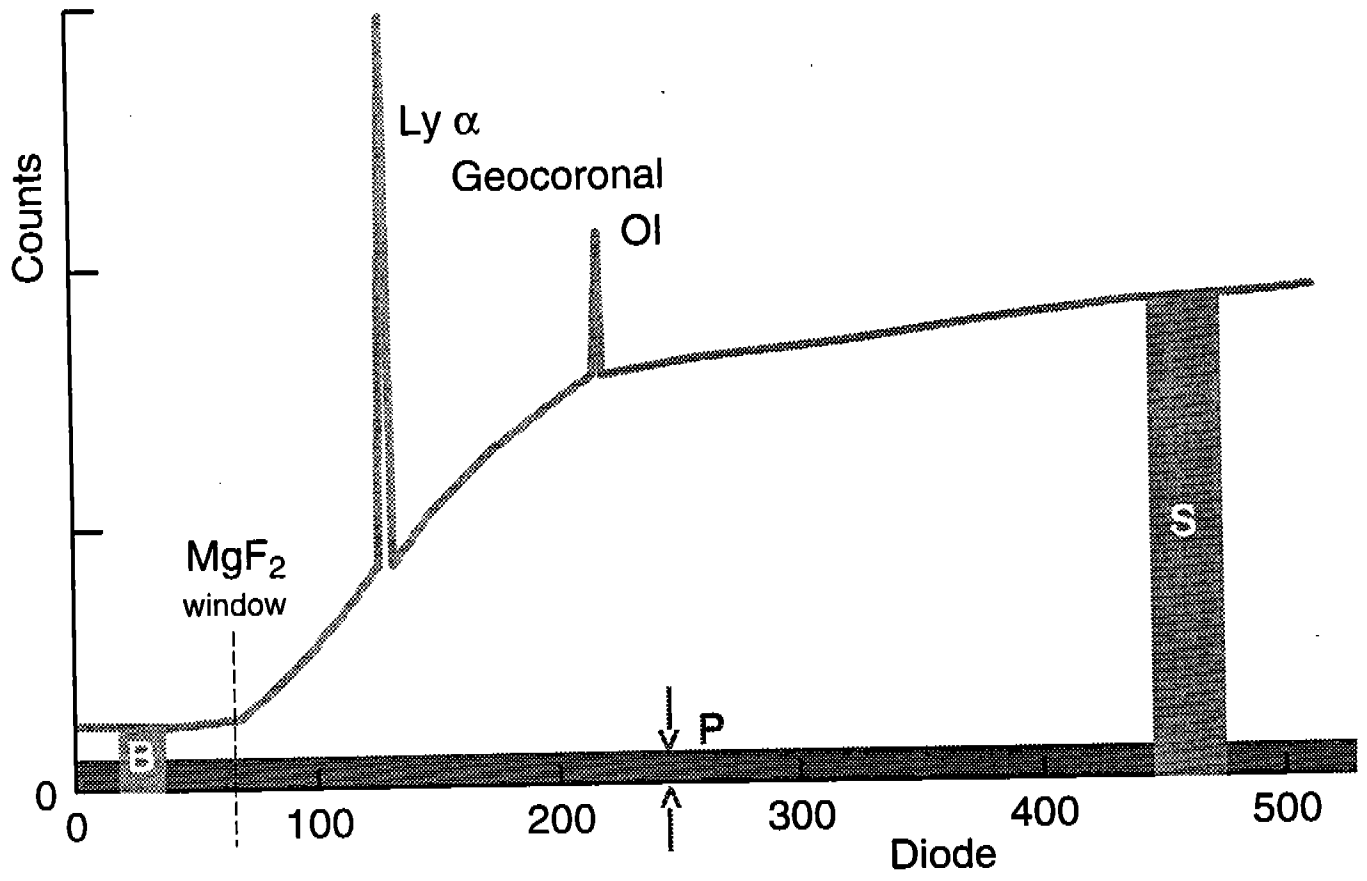


Fig. 1

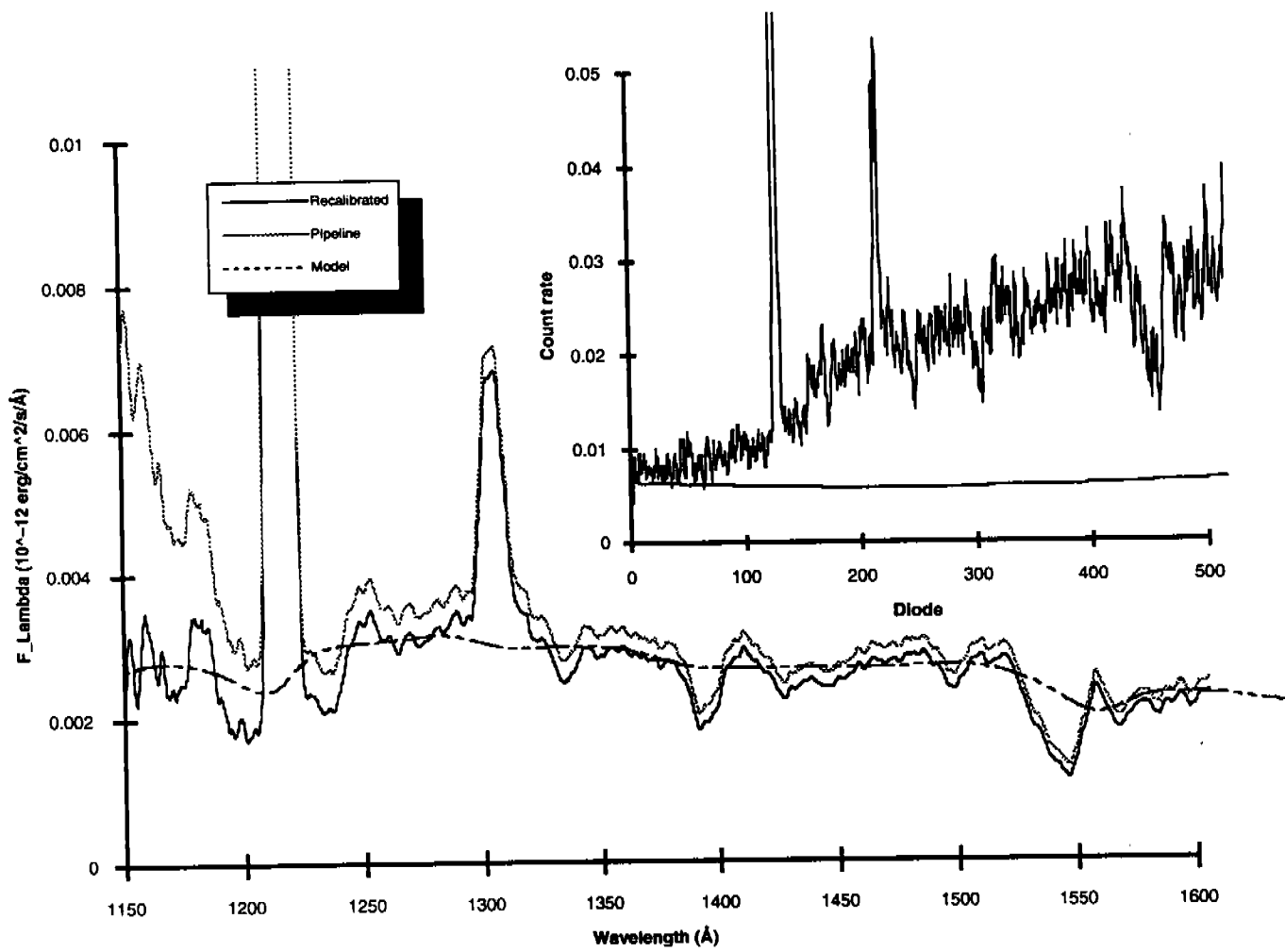


Fig. 2

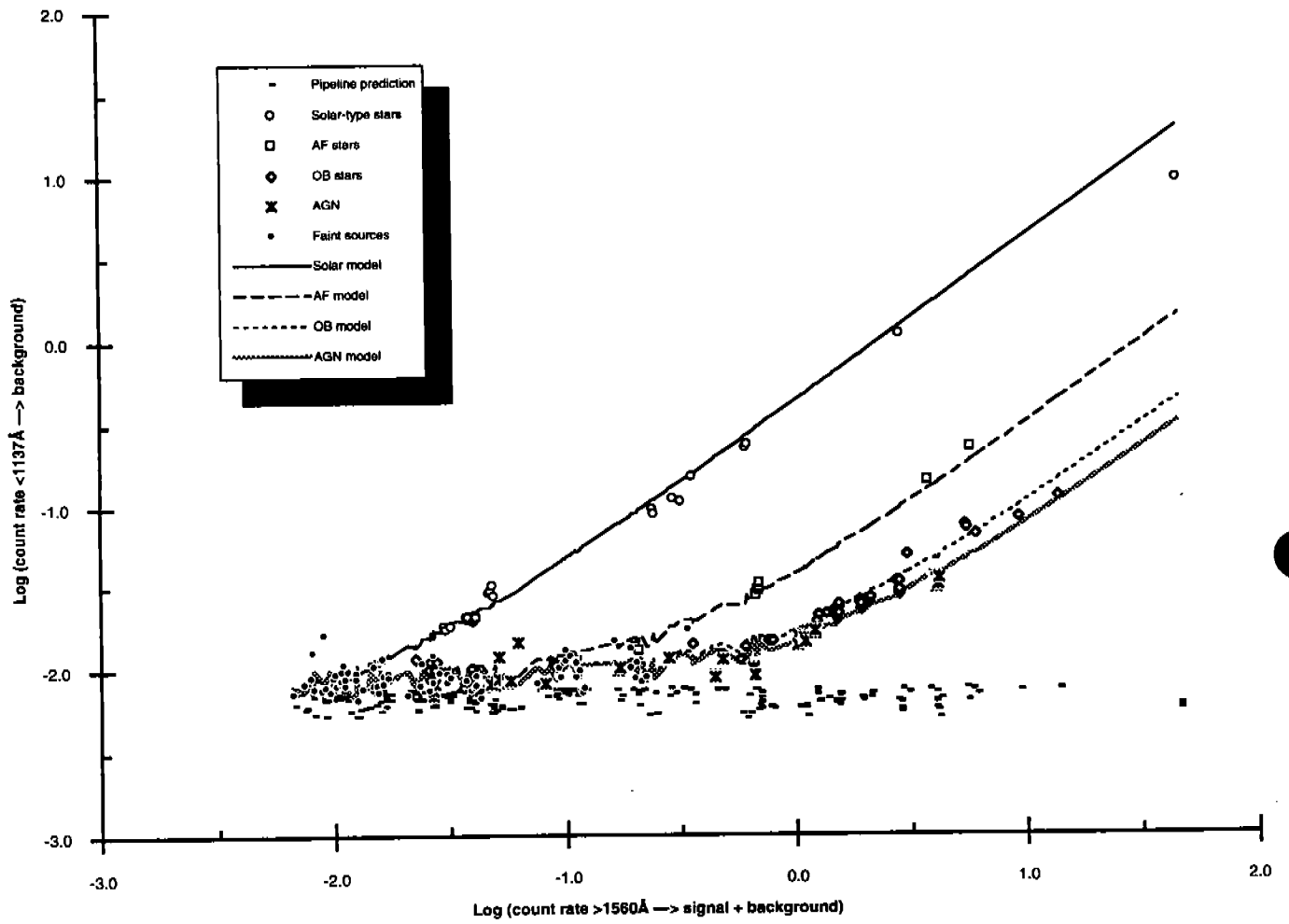


Fig. 3

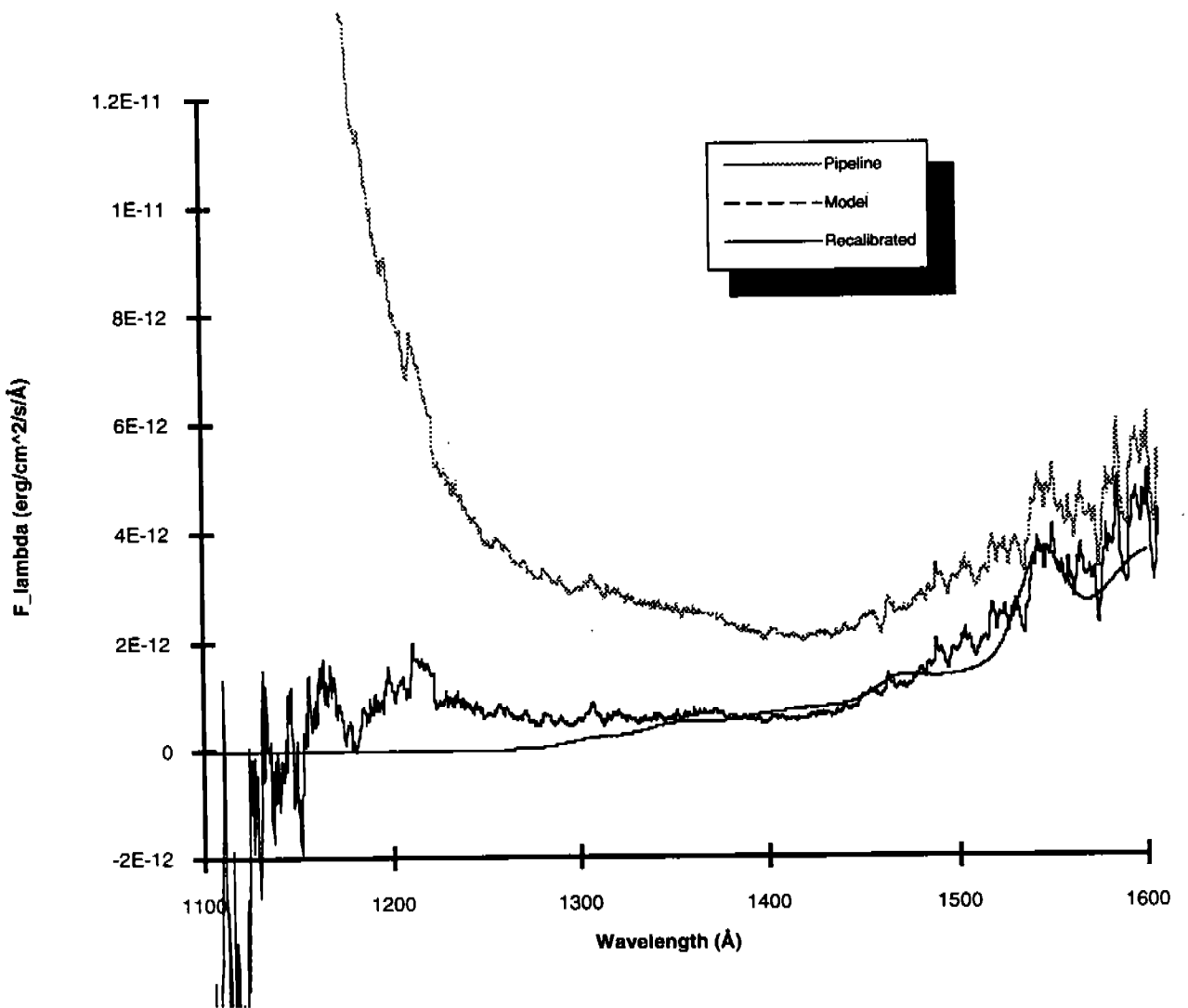


Fig. 4

